

1 **Contribution of riverine dissolved organic carbon to organic carbon**
2 **decomposition in the Ariake Sea, Japan, a coastal area suffering from**
3 **summer hypoxia**

4
5 **Hiroyuki Takasu** ^{1,2,3*}, **Tomohiro Okamura** ^{2,4}, **Tomohiro Komorita** ⁵, **Tomohiro**
6 **Shiragaki** ², **Koji Uchino** ^{2,6}

7
8 *¹Faculty of Environmental Science, Nagasaki University, 1-14 Bunkyo-machi, Nagasaki,*
9 *852-8521, Japan*

10 *²Graduate School of Fisheries and Environmental Sciences, Nagasaki University, 1-14*
11 *Bunkyo-machi, Nagasaki, 852-8521, Japan*

12 *³Division of Marine Energy Utilization, Organization for Marine Science and*
13 *Technology, Nagasaki University, 1-14 Bunkyo-machi, Nagasaki, 852-8521, Japan*

14 *⁴National Research Institute of Fisheries and Environment of Inland Sea, Japan*
15 *Fisheries Research and Education Agency, 2-17-5, Maruishi, Hatsukaishi, Hiroshima,*
16 *739-0452, Japan*

17 *⁵Faculty of Environmental and Symbiotic Science, Prefectural University of Kumamoto,*
18 *3-1-100 Tsukide, Kumamoto, 862-8502, Japan*

19 *⁶Kyushu Environmental Evaluation Association, 1-10-1 Matsukadai, Higashi-ku,*
20 *Fukuoka, 813-0004, Japan*

21
22 * Corresponding author: takasu@nagasaki-u.ac.jp

23 Telephone & Fax number: +81-95-819-2752

24
25 Key words: Dissolved organic carbon; riverine organic matter; hypoxia; carbon stable
26 isotope ratio

27 **Statements and declarations**

28 The authors declare that they have no known competing financial interests or
29 personal relationships that could have appeared to influence the work reported in this
30 paper.

31

32 **Data availability**

33 The datasets of this study may be available from the corresponding author on
34 request.

35

36

37

38 **Abstract**

39 Dissolved organic carbon (DOC) comprises nearly half of the riverine organic
40 carbon flux into oceans. Although riverine DOC is involved in numerous important
41 ecosystem functions, excessive labile DOC inputs from rivers may contribute to
42 hypoxia in coastal systems. Furthermore, many aspects of the contribution of riverine
43 DOC to hypoxia are unknown. The natural carbon stable isotope ratio ($\delta^{13}\text{C}$) in organic
44 matter can be used to identify sources of organic carbon in coastal oceans. In this study,
45 we analyzed the concentrations and $\delta^{13}\text{C}$ values of DOC in the bottom layer of the
46 northern Ariake Sea, Japan, in which hypoxic water develops during summer.
47 Additionally, we compared the $\delta^{13}\text{C}$ values of DOC at the beginning and end of an
48 incubation experiment to determine the contribution of riverine DOC decomposition to
49 hypoxia. The results of this study indicate that the bottom DOC concentration is
50 influenced by both phytoplankton and river water, with the former likely having a
51 stronger impact in the northwestern Ariake Sea in summer. Nevertheless, we also found
52 major contributions ($\sim 49.7\%$) of DOC decomposition to total organic carbon
53 decomposition at some stations. The initial $\delta^{13}\text{C}$ value of DOC ranged from -24.0% to
54 -22.2% , and the DOC $\delta^{13}\text{C}$ increased (from $+0.3\%$ to $+0.8\%$) in three of the five
55 incubation bottles after incubation. This might be caused by selective decomposition of
56 ^{13}C -depleted organic matter. The decomposed DOC in those bottles must be mainly
57 derived from terrestrial sources. This result implies that riverine DOC decomposition
58 contributes to hypoxia formation in the bottom layer of the northern Ariake Sea.

59

60

61 **1. Introduction**

62 Dissolved organic carbon (DOC) represents the largest pool of reduced carbon
63 in oceans and plays important roles in the ocean carbon cycle and food webs (Hansell
64 and Carlson 2002). DOC comprises nearly half of the riverine organic carbon flux into
65 oceans (Dai et al. 2012). Riverine DOC is involved in numerous ecosystem functions,
66 including key roles in chemical and biological processes. Refractory and labile DOC are,
67 respectively, important for carbon sequestration in the ocean (Jiao et al. 2014) and a
68 vital food source for marine bacteria (Asmala et al. 2013; 2014).

69 The frequency of hypoxia ($< 2\text{--}3 \text{ mg O}_2 \text{ L}^{-1}$, Chen et al. 2007; Diaz and
70 Rosenberg 2008) resulting from eutrophication in coastal systems has increased since
71 the 1960s (Diaz and Rosenberg 2008). Excessive labile organic matter inputs from
72 rivers also contribute to hypoxia in aquatic systems (DeVilbiss et al. 2016). Although
73 riverine DOC is considered less bioavailable to marine bacteria than marine DOC
74 produced by marine phytoplankton, many aspects regarding the contribution of riverine
75 DOC to hypoxia remain unknown, as exemplified by the limited research conducted on
76 this topic (Deutsch et al. 2012). Several studies have suggested that riverine DOC is
77 more bioavailable to marine bacteria than previously thought (Rochelle-Newall et al.
78 2004; Bianchi 2007; Ward et al. 2013; Takasu and Uchino 2021). Based on that finding,
79 we hypothesize that DOC exported from rivers contributes to oxygen consumption at
80 the bottom of the water column in coastal systems. Based on our hypothesis, we
81 predicted that DOC in the bottom water contains a river-derived component that will
82 decrease after a certain incubations time. However, the aforementioned studies were
83 mostly conducted in surface seawater (Rochelle-Newall et al. 2004; Takasu and Uchino

84 2021), whereas the freshness of organic matter differs between the surface and bottom
85 layers (Yamashita and Tanoue 2003). Therefore, there are no quantification of riverine
86 DOC to total organic matter decomposition in bottom water and to hypoxia formation.

87 The stable carbon isotope ($\delta^{13}\text{C}$) of DOC can be used to identify sources of DOC
88 in coastal oceans (Raymond and Bauer 2001). Because terrestrial and marine DOC
89 produced by marine phytoplankton are isotopically distinct (Peterson et al. 1994), the
90 $\delta^{13}\text{C}$ value of a given DOC sample enables the relative contributions of riverine and
91 marine DOC to be estimated (Raymond and Bauer 2001). The solid-phase extraction
92 (SPE) method established by Dittmar et al. (2008), using a styrene-divinylbenzene
93 polymer (PPL), is now commonly used to isolate DOC from seawater salts for
94 molecular and isotopic analyses. Extraction efficiency is 20-62% of total DOC in
95 natural water samples (Chen et al. 2016; Dittmar et al. 2008). Although some studies
96 have reported that PPL can extract a representative proportion of dissolved organic
97 matter (DOM) (Broek et al. 2017; Dittmar et al. 2008), other work has shown that there
98 may be selectivity in DOM extracted by PPL (Chen et al. 2016). Therefore, caution may
99 need to be paid on studies using DOM extracted by PPL. However, the extracted DOC
100 by PPL may be a powerful method for stable isotope analysis of DOM (Broek et al.
101 2017; Lewis et al. 2020). The DOC $\delta^{13}\text{C}$ data derived from SPE method could be used
102 to quantify riverine DOC supply and its degradation in bottom water.

103 The Ariake Sea is located off central Kyushu Island and is one of the most
104 productive semi-enclosed bays of Japan. Since the second half of the 1990s, severe
105 summer hypoxia has occurred frequently in the northern part of the Ariake Sea
106 (Tsutsumi et al. 2015). Hayami and Fujii (2018) suggested that the decadal-scale
107 progressive increase in hypoxia in the inner part of the Ariake Sea is caused by

108 increased oxygen consumption due to enhanced organic matter fluxes into the bottom
109 water. At the northern part of the Ariake Sea, the bottom dissolved oxygen (DO)
110 concentration decreases from spring tide to neap tide (Hayami 2007). When the
111 stratification becomes stronger, the hypoxia occurs from half tide to neap tide due to
112 rapid oxygen consumption by organic matter decomposition even at shallow marginal
113 areas of tidal flat during summer season (Hayami 2007). Thus, elucidation of sources of
114 labile organic matter in the bottom layer is essential to understand the mechanism of
115 hypoxia formation in this area. Although the decomposition of sediment organic carbon
116 and particulate organic carbon (POC) are the dominant processes for oxygen
117 consumption (Tokunaga et al., 2005), we previously found that DOC decomposition
118 contributes to hypoxia formation (Uchino et al. 2019). In addition, we found that
119 terrestrial DOM distributed in the bottom throughout the northern part of the Ariake Sea
120 (Uchino et al. 2021). However, the contribution of terrestrial DOC decomposition to
121 hypoxia formation is still unknown.

122 The Chikugo River is the largest river discharging into the Ariake Sea. We
123 recently reported that the Chikugo River is the primary source of riverine DOC in the
124 northern Ariake Sea (Uchino et al. 2021). Our previous study also suggested that
125 riverine DOC from the Chikugo River is more bioavailable to marine bacteria in the
126 surface water than previously thought (Takasu and Uchino 2021). However, the extent
127 of the contribution of DOC exported from the Chikugo River to oxygen consumption at
128 the bottom of the water column in the northern Ariake Sea is still unknown.

129 To test the hypothesis that the terrestrial DOC contributes hypoxic water
130 formation of the bottom layer, we analyzed the DOC concentrations and $\delta^{13}\text{C}$ values of
131 DOC, derived using the SPE method (Dittmer et al. 2008), from the bottom layer of the

132 northern Ariake Sea, in which hypoxic water forms during summer. Additionally, we
133 compared the $\delta^{13}\text{C}$ values of DOC at the beginning and end of an incubation experiment
134 to determine the contribution of riverine DOC decomposition to summer hypoxia.

135

136 **2. Methods**

137 *2.1. Sampling*

138 In 2019, we conducted a preliminary investigation to confirm whether a riverine
139 DOC signature can be identified based on $\delta^{13}\text{C}$ values of DOC in the bottom layer of the
140 northern Ariake Sea. Because organic matter discharged from the Chikugo River
141 accumulate around the northwestern part of the Ariake Sea, seawater samples were
142 collected from May to August at two stations located in the northwestern part of the bay
143 (Fig. 1). Because the hypoxia occurs from half tide to neap tide, samplings were
144 conducted during spring tide to collect fresh DOC before extensive microbial
145 decomposition. The water temperature, salinity, and seawater density ($\sigma\text{-t}$) were
146 measured at 1 m above the sea bottom using a multi-parameter water quality meter
147 (WQC-24; DKK-TOA, Tokyo, Japan). Seawater samples were collected at 1 m above
148 the sea bottom at each station using a 3-L Van Dorn water sampler (RIGO, Tokyo,
149 Japan). Samples for dissolved oxygen (DO) and chlorophyll *a* (Chl. *a*) analysis were
150 drained into 100-mL biological oxygen demand bottles and 125-mL amber polyethylene
151 bottles, respectively. Seawater samples used for DOC concentration analysis were
152 filtered onboard the ship using pre-combusted 0.7- μm GF/F filters (General Electric,
153 Coventry, UK) and stored in new acid-washed 125-mL high-density polyethylene
154 bottles. Filtrates for DOC analysis were stored at -20°C until further analysis. Seawater

155 samples used for the analysis of POC concentrations and $\delta^{13}\text{C}$ values of DOC and POC
156 were poured into aged acid-washed 10-L polycarbonate tanks.

157 In 2020, water samples were collected at five stations located in the northern
158 Ariake Sea from the mouth of the Chikugo River to the opposite shore (Fig. 1) on
159 August 29. This transect was selected considering the behavior of freshwater, which
160 flows from the Chikugo River toward the inner Ariake Sea (Ishita et al. 2016). The
161 Chikugo river flows into the northern Ariake Sea at an annual average flow rate of
162 $115.1 \text{ m}^3 \text{ s}^{-1}$ (Sato and Takita 2000). Although the Rokkaku River (annual average flow
163 rate, $4.36 \text{ m}^3 \text{ s}^{-1}$) (Japan River Association 2020) and the Shiota River (average flow
164 rate prior to the rainy season calculated from dam discharges, $0.55 \text{ m}^3 \text{ s}^{-1}$) (Ministry of
165 Land 2020a; 2020b) also discharge into the northern Ariake Sea, the flow rates of those
166 rivers are much lower than that of the Chikugo River. Sampling was conducted during
167 the ebb phase of a spring tide. The water temperature, salinity, and seawater density
168 ($\sigma\text{-t}$) were measured at 0.5–1-m depth intervals from the sea surface to the bottom
169 using the multi-parameter water quality meter. Seawater samples were collected from
170 three or four depths at each station using a 3-L Van Dorn water sampler for analyzing
171 DO and Chl. *a* concentrations. Samples for an incubation experiment were collected at 1
172 m above the sea bottom at each station and poured into aged acid-washed 10-L
173 polycarbonate tanks. Polyvinyl chloride gloves were worn during sample collection and
174 processing to avoid contamination.

175

176 *2.2. Experiments on organic matter decomposition*

177 To determine the contribution of riverine DOC decomposition to hypoxic water
178 formation, the $\delta^{13}\text{C}$ values of DOC at the beginning and end of an incubation

179 experiment were compared. Water samples were well-mixed for aeration and poured
180 into acid-washed 5-L glass bottles and incubated for 7 days at the *in-situ* temperature
181 (27°C for Sts. A and B, and 25 °C for Sts. C, D and E) with shaking using orbital
182 shakers (SHK-U4, AGC TECHNO GLASS Co., Ltd., Shizuoka, Japan, shaking speed
183 of 100 rpm) in darkness. The concentrations and $\delta^{13}\text{C}$ values of DOC and POC were
184 determined before and after incubation. The experiment could not be replicated due to a
185 limitation in space available for incubation. To mimic natural environmental conditions,
186 the particulate fraction was not removed via filtration.

187

188 2.3. Chemical and biological analyses

189 Concentrations of DO were measured with the Winkler titration method
190 (Dickson 1994) using an automated titration system (AT-710; Kyoto Electronics, Kyoto,
191 Japan). Chl. *a* concentrations were determined from sample residues collected on GF/F
192 filters, extracted with *N, N*-dimethylformamide (Fujifilm Wako Pure Chemical
193 Industries, Osaka, Japan), and analyzed using fluorometry (FP-8300; JASCO, Tokyo,
194 Japan) according to the method of Welschmeyer (1994). DOC concentrations were
195 determined using a total carbon analyzer (TOC-V; Shimadzu, Kyoto, Japan). A
196 calibration curve was obtained by analyzing four distinct concentrations of a standard
197 solution prepared from potassium hydrogen phthalate. As a procedural blank, ultrapure
198 water (Milli-Q, Direct-Q UV3; Merck Millipore, Burlington, MA, USA) was analyzed
199 every 10 samples, and the average pooled peak area from Milli-Q water analysis over
200 the entire day was subtracted from the seawater sample peak areas. The analytical
201 accuracy of the standard solution was less than 5%. To determine the $\delta^{13}\text{C}$ values of
202 DOC, DOC was extracted and concentrated using the PPL-SPE method (Dittmar et al.

203 2008) on the day of collection. PPL-SPE cartridges (Bond Elut-PPL 500 mg 6 mL;
204 Agilent, Santa Clara, CA, USA) were activated with methanol (LC/MS grade; Fujifilm
205 Wako, Tokyo, Japan) and rinsed with Milli-Q water that had been acidified to 0.01 M
206 H⁺. The cartridges were loaded with acidified GF/F filtrate samples at a flow rate of 40
207 mL min⁻¹ using new acid-washed Teflon tubing by a peristaltic pump (Masterflex
208 tubing pump system L/S; Masterflex, Gelsenkirchen, Germany). Three-liter of acidified
209 samples were loaded to the cartridges in 2019 experiment. By contrast, sample volume
210 was increased to 5-L in 2020 experiment because relatively low DOC concentrations
211 were predicted after incubation. Cartridges were dried for 30 min under ultra-pure N₂
212 gas, and the SPE-derived DOC was then eluted with 6 mL methanol. The eluted
213 methanol was dried again under ultra-pure N₂ gas, and the residues were stored at
214 -20°C until further analysis. To determine POC concentrations and δ¹³C values of POC,
215 sample residues collected on precombusted GF/F filters were fumed with HCl to
216 remove carbonate salts, neutralized, and dried in a desiccator (Lorrain et al. 2003).
217 Samples and standards were individually wrapped in tin foil (Tin foil Squares; Säntis
218 Analytical AG, Teufen, Switzerland) before analysis. The δ¹³C values of DOC and
219 POC as well as POC concentrations were analyzed using an elemental analyzer
220 equipped with a stable isotope ratio mass spectrometer (Flash 2000/Conflo IV/DELTA
221 V Advantage; Thermo Fisher Scientific, Bremen, Germany) at Atmosphere and Ocean
222 Research Institute of The University of Tokyo. The C isotope ratio is reported using
223 conventional δ -notation (δ¹³C) with Vienna Pee Dee Belemnite (VPDB) as reference
224 standards. Stable isotope ratios are expressed as the per mil (‰) deviation from the
225 international standard using the following equation: $\delta X = [(R_{\text{sample}}/R_{\text{standard}}) - 1] \times 1000$,

226 where X and R represent ^{13}C and the $^{13}\text{C}/^{12}\text{C}$ ratio in this study, respectively. L-alanine
227 (-19.6% ; SI-Science, Tokyo, Japan) was used as working standard for calibration.

228

229 2.4. Data analysis and statistical analysis

230 Applying the two-source linear mixing model with $\delta^{13}\text{C}$, the mass balance for
231 the carbon isotope is,

$$232 \quad \delta^{13}\text{C}_m = R_x\delta^{13}\text{C}_x + R_y\delta^{13}\text{C}_y \quad (1)$$

$$233 \quad 1 = R_x + R_y \quad (2)$$

234 where $\delta^{13}\text{C}$ represents the $\delta^{13}\text{C}$ values, and the subscripts x , y , and m represent
235 two sources and a mixture, respectively. R_x and R_y represent the fractional contribution
236 rate of $\delta^{13}\text{C}$ from each source to mixture. Using the mixing model, the relative
237 contribution of terrestrial organic matter (R_{terr}) and phytoplankton (R_{phy}) to the mixture
238 (POC and DOC) were calculated from the following equations.

$$239 \quad R_{\text{terr}} (\%) = (\delta^{13}\text{C}_{\text{phy}} - \delta^{13}\text{C}_m) / (\delta^{13}\text{C}_{\text{phy}} - \delta^{13}\text{C}_{\text{terr}}) \quad (3)$$

$$240 \quad R_{\text{phy}} (\%) = (\delta^{13}\text{C}_{\text{terr}} - \delta^{13}\text{C}_m) / (\delta^{13}\text{C}_{\text{terr}} - \delta^{13}\text{C}_{\text{phy}}) \quad (4)$$

241 where $\delta^{13}\text{C}_{\text{terr}}$ and $\delta^{13}\text{C}_{\text{phy}}$ are the $\delta^{13}\text{C}$ values for the terrestrial organic matter and
242 phytoplankton, respectively. The end-member compositions, $\delta^{13}\text{C}_{\text{terr}}$ and $\delta^{13}\text{C}_{\text{phy}}$ that
243 were assumed to be -28.5 and -19.7% , respectively (Yoshino et al. 2018).

244 Pearson correlation analysis was performed to identify the sources of DOC and
245 POC using the “corr()” function in R ver. 3.3.3 (R Development Core Team, 2017).

246

247 **3. Results**

248 *3.1. Physicochemical parameters and concentrations and $\delta^{13}\text{C}$ values of DOC and POC*
249 *in the bottom layer of the northwestern Ariake Sea in 2019*

250 In the bottom layer of the northwestern Ariake Sea, the salinity at Sts. 1 and 2
251 was always lower than 30, with respective ranges of 21.3–28.0 (average \pm standard
252 deviation [SD]: 26.3 ± 3.3) and 25.4–29.6 (average \pm SD: 27.9 ± 1.8), respectively
253 (Table 1). The DO ranges at Sts. 1 and 2 were in the range of 2.3–5.6 mg L^{-1} (average \pm
254 SD: $3.9 \pm 1.3 \text{ mg L}^{-1}$) and 3.3–6.3 mg L^{-1} (average \pm SD: $4.8 \pm 1.4 \text{ mg L}^{-1}$), respectively
255 (Table 1). Hypoxic water mass (2.3 mg L^{-1}) was found at St. 1 in August (Table 1). The
256 Chl. *a* concentrations at Sts. 1 and 2 were fell within the ranges of 5.2–15.9 $\mu\text{g L}^{-1}$
257 (average \pm SD: $9.7 \pm 4.6 \mu\text{g L}^{-1}$) and 10.6–15.2 $\mu\text{g L}^{-1}$ (average \pm SD: $12.0 \pm 2.2 \mu\text{g L}^{-1}$),
258 respectively (Table 1).

259 The DOC concentration ranges at Sts. 1 and 2 were 102.4–132.4 $\mu\text{mol L}^{-1}$
260 (average \pm SD: $121.6 \pm 13.1 \mu\text{mol L}^{-1}$) and 79.9–145.7 $\mu\text{mol L}^{-1}$ (average \pm SD: $114.9 \pm$
261 $34.0 \mu\text{mol L}^{-1}$), respectively (Table 1), whereas the respective POC concentration
262 ranges were 22.5–57.5 $\mu\text{mol L}^{-1}$ (average \pm SD: $39.1 \pm 14.7 \mu\text{mol L}^{-1}$) and 22.5–40.0
263 $\mu\text{mol L}^{-1}$ (average \pm SD: $30.2 \pm 7.5 \mu\text{mol L}^{-1}$) (Table 1). Concentrations of DOC were
264 much higher than those of POC in the bottom layer of the northwestern Ariake Sea
265 during summer. The DOC $\delta^{13}\text{C}$ values at Sts. 1 and 2 ranged from -23.9‰ to -23.0‰
266 (average \pm SD: $-23.3 \pm 0.4 \text{‰}$) and from -24.7‰ to -22.7‰ (average \pm SD: $-23.6 \pm$
267 0.8‰), respectively (Table 1), whereas the POC $\delta^{13}\text{C}$ values ranged from -26.7‰ to
268 -24.6‰ (average \pm SD: $-25.4 \pm 0.9 \text{‰}$) and from -24.3‰ to -22.6‰ (average \pm SD:
269 $-23.5 \pm 0.8 \text{‰}$), respectively (Table 1). The rates of contribution of terrestrial organic

270 matter to DOC at Sts. 1 and 2 ranged from 37.6% to 47.7% (average \pm SD: $41.2 \pm$
271 4.49%) and from 34.1% to 56.8% (average \pm SD: $44.3 \pm 9.42\%$), respectively (Table 1),
272 whereas the rates of contribution of terrestrial organic matter to POC ranged from
273 55.7% to 79.5% (average \pm SD: $64.8 \pm 10.8\%$) and from 33.0% to 52.3% (average \pm
274 $SD: 42.6 \pm 9.39\%$), respectively (Table 1).

275

276 *3.2. Physicochemical parameters for the northern Ariake Sea in 2020*

277 In the northern Ariake Sea, the ranges for water temperature and salinity were
278 $24.7\text{--}28.4^\circ\text{C}$ (average \pm SD: $26.6 \pm 1.34^\circ\text{C}$) and $23.5\text{--}28.0$ (average \pm SD: 26.0 ± 1.26),
279 respectively (Fig. 2). Water temperature decreased with increasing water depth, whereas
280 salinity increased with increasing water depth. As a result, sigma- t increased with
281 increasing depth (Fig. 2). Differences of sigma- t between the surface and bottom layers
282 were remarkable at deeper sites (Sts .C and D) (Fig. 2). The DO concentration ranged
283 from 2.41 to 10.7 mg L^{-1} (average \pm SD: $5.7 \pm 2.33 \text{ mg L}^{-1}$), and hypoxic water masses
284 featuring DO levels of less than 3 mg L^{-1} were found in the bottom layer at Sts. C and D
285 (Fig. 2). The Chl. a concentration ranged from 0.38 to $5.74 \text{ }\mu\text{g L}^{-1}$ (average \pm SD: $4.0 \pm$
286 $1.72 \text{ }\mu\text{g L}^{-1}$).

287 DOC and POC concentrations were not significantly correlated with salinity or
288 the Chl. a concentration ($p > 0.05$) in 2019. In 2020, a significant positive correlation
289 was found between the Chl. a concentration and the initial DOC concentration ($r^2 =$
290 0.81 , $p < 0.05$, Fig. 3). Conversely, a negative correlation was found between salinity
291 and the DOC concentration, although it was marginally significant ($r^2 = 0.67$, $p = 0.091$
292 Fig. 3).

293

294 3.3. Changes in concentrations and $\delta^{13}\text{C}$ values of DOC and POC before and after
295 incubation

296 In the organic carbon decomposition experiment, the initial concentrations of
297 DOC (average \pm SD: $112.9 \pm 16.0 \mu\text{mol L}^{-1}$) were higher than those of POC (average \pm
298 SD: $74.1 \pm 36.3 \mu\text{mol L}^{-1}$) except for St.A (Table 2a). However, at the end of the
299 incubation experiment, the decreased DOC concentrations (average \pm SD: 3.3 ± 2.1
300 $\mu\text{mol L}^{-1}$) were much lower than those of the POC (average \pm SD: $21.1 \pm 12.8 \mu\text{mol L}^{-1}$).
301 The contribution of DOC decomposition to total organic carbon (sum of DOC and
302 POC) decomposition ranged from 0% to 49.7% (average \pm SD: $20.1 \pm 19.2\%$), the
303 initial $\delta^{13}\text{C}$ value of DOC ranged from -24.0% to -22.2% (average \pm SD: $-25.4 \pm$
304 0.9%) (Table 2b). After incubation, the DOC $\delta^{13}\text{C}$ increased in three of the five
305 incubation bottles (from $+0.3\%$ to $+0.8\%$, Table 2b, Fig. 4). The initial $\delta^{13}\text{C}$ value of
306 POC ranged from -26.6% to -20.9% (average \pm SD: $-23.6 \pm 2.1 \%$) (Table 2b, Fig. 4).
307 In contrast to the DOC $\delta^{13}\text{C}$, the POC $\delta^{13}\text{C}$ decreased drastically in four of the five
308 incubation bottles (-2.5% - 5.2% , Table 2b, Fig. 4). Based on the mixing model results,
309 the relative contribution of terrestrial organic matter to DOC at initial and final of
310 incubations ranged from 28.4% to 48.9% (average \pm SD: $40.2 \pm 9.0\%$) and from 36.4%
311 to 45.5% (average \pm SD: $40.9 \pm 3.5\%$), respectively (Table 2), whereas the relative
312 contribution of terrestrial organic matter to POC at initial and final of incubations
313 ranged from 13.6% to 78.4% (average \pm SD: $43.9 \pm 24.0\%$) and from 61.4% to 93.2%
314 (average \pm SD: $76.6 \pm 11.5\%$), respectively (Table 1).
315

316 **4. Discussion**

317 *4.1. Source of DOC in the bottom layer of the northern Ariake Sea*

318 In the northwestern Ariake Sea, the salinity was always lower than 30 (Table 1,
319 Fig. 2), indicating a continuous inflow of river water that was distributed throughout all
320 layers of the bay. The results of correlation analysis (Fig. 3) indicate that the bottom
321 DOC concentration is influenced by both phytoplankton exudates and river water, with
322 the former likely having a stronger impact. This interpretation is supported by the $\delta^{13}\text{C}$
323 values of the bottom DOC (Tables 1 and 2). In the Ariake Sea, the $\delta^{13}\text{C}$ value of
324 riverine particulate organic matter ranges from -28.5‰ to -27.2‰ , whereas that for
325 marine phytoplankton ranges from -21.8‰ to -19.7‰ (Yoshino et al. 2018). These
326 values are similar to the typical $\delta^{13}\text{C}$ values of freshwater DOC (-28.8‰ to -27.9‰ ;
327 Raymond and Bauer 2001) and marine DOC (-23.0‰ to -18.0‰ ; Raymond and Bauer
328 2001; Bauer 2002) in temperate regions. The DOC $\delta^{13}\text{C}$ values in both 2019 and 2020
329 were similar to the $\delta^{13}\text{C}$ values for marine phytoplankton in the Ariake Sea (Tables 1
330 and 2). For DOC, the relative contributions of phytoplankton were always higher than
331 that of terrestrial organic matter (Table 1, 2). Although POC concentrations were not
332 significantly correlated with salinity and the Chl. *a* concentrations (Fig. 3), the relative
333 contributions of phytoplankton to POC tended to be higher than that of terrestrial
334 organic matter (Table 1, 2). These results support the aforementioned interpretation of
335 the influence of phytoplankton and are consistent with a report for another coastal area
336 that experiences summer hypoxia (Zhang et al. 2018).

337

338

339 4.2. Contribution of riverine DOC to hypoxia

340 The amounts of DOC decomposition were relatively constant except for St.A
341 (3.3-5.8 $\mu\text{mol L}^{-1}$, Table 2a). Although the experiment could not be replicated, previous
342 study has reported similar values in the northern part of the Ariake Sea (2.9-7.6 $\mu\text{mol L}^{-1}$, Uchino et al. 2019). In this study, the particulate fraction was not removed via
343 filtration for the DOC decomposition experiment. A previous study reported that when
344 POC derived from phytoplankton was incubated with a bacterial inhibitor (formalin or
345 HgCl_2) at 18°C, 26–29% of the carbon was lost as DOC within 24 h of the incubation
346 start time (Lee and Fisher 1992). Therefore, it should be noted that our estimates of
347 DOC decomposition are likely conservative, because the decreases in DOC might have
348 been masked by DOC leaching from POC decomposition. Nevertheless, the
349 contribution of DOC decomposition to total organic carbon decomposition was not
350 negligible (average \pm SD: 20.1 \pm 19.2%) except for St.A where highest POC
351 decomposition was observed. Thus, DOC decomposition may contribute to hypoxia
352 formation in the northern part of the Ariake Sea. Regardless of the source of DOC, the
353 amount of DOC decomposition was relatively constant compared to that of POC
354 decomposition (Table 2a), and the contribution of DOC decomposition to total organic
355 carbon decomposition was large when POC decomposition was low (Table 2a). Amount
356 of POC decomposition seem to result in differences of the ratio of DOC decomposition
357 to total organic carbon decomposition among stations. The contributions of marine and
358 terrestrial POC to total POC varied (13.6 – 78.4%, Table 2b). Nevertheless, the initial
359 concentrations of POC were positively correlated with the POC decomposition rates,
360 although it was marginally significant ($r = 0.81$, $p = 0.096$). Thus, labile fraction of
361 POC in both marine and terrestrial origin might be selectively decomposed during the 7-

363 days incubation, and the amount of labile POC might be controlled by the total amount
364 of POC rather than its origin in this study.

365 Assuming the Redfield ratio (based on $O_2/C = 1.30$, Redfield et al. 1963), the
366 estimated oxygen consumption rate due to total organic carbon decomposition rates
367 ranged from 0.5 to 1.4 mg $O_2 L^{-1}$ (average \pm SD: 1.02 ± 0.48 mg $O_2 L^{-1}$), and the
368 decomposition rate for only DOC ranged from 0 to 0.24 mg $O_2 L^{-1}$ (average \pm SD: 0.14
369 ± 0.09 mg $O_2 L^{-1}$). Previous study reported that weekly oxygen consumption rate in this
370 area during summer season were around 2 mg $O_2 L^{-1}$ (Uchino et al. 2019). Because
371 oxygen consumption rate via organic matter decomposition is not sufficient to explain
372 the weekly oxygen consumption, bottom hypoxia might be caused by not only organic
373 matter decomposition but also by chemical oxygen consumption of the reducing
374 substances (Tokunaga et al. 2016). It is important to note that estimated oxygen
375 consumptions may contain predicted errors, because Redfield ratio is not applicable to
376 terrestrial organic matter. However, the role of DOC decomposition seemed to be non-
377 negligible.

378 Although the initial $\delta^{13}C$ values of POC and DOC would be the initial conditions
379 representing the influence of freshwater from the Chikugo River versus marine organic
380 matter, no systematic changes of the $\delta^{13}C$ values of POC and DOC have been found
381 along the transect (Table 2b). POC and DOC showed the lowest $\delta^{13}C$ values at St.A
382 (Table 2A), suggesting the strong influence of riverine fresh organic matter in this site.
383 At the end of the incubation experiment, differences of the $\delta^{13}C$ values of POC and
384 DOC among stations became small (Table 2A). At the end of the incubation experiment,
385 most POC $\delta^{13}C$ values had decreased (Table 2b, Fig. 4). Theoretically, selective
386 decomposition of marine DOC, which is enriched in ^{13}C , results in an overall lighter ^{13}C

387 signature in the DOC remaining at the end of the incubation (Lehmann et al. 2002).
388 Thus, decomposed POC must be mainly derived from marine sources. However, ~88%
389 of POC was decomposed during the incubation period at St. A (from 42.5 to 5.0 μmol
390 L^{-1}), though no corresponding change in the POC $\delta^{13}\text{C}$ was observed (from -26.6‰ to -
391 26.5‰). Therefore, marine and fresh riverine POC might be equally decomposed during
392 the incubation period at St. A. In contrast to POC, the DOC $\delta^{13}\text{C}$ values increased in
393 three of five incubation bottles (Table 2b, Fig. 4). This might be caused by selective
394 decomposition of ^{13}C -depleted organic matter. Thus, decomposed DOC in those bottles
395 must be mainly derived from terrestrial sources. This result implies that riverine DOC
396 decomposition contributes to total DOC decomposition in the bottom layer of the
397 northern Ariake Sea.

398 Previous study has reported that the bioavailability of high-molecular-weight
399 DOM extracted by ultrafiltration was comparable between the river and marine site in
400 the northern part of the Ariake Sea (Takasu and Uchino 2021). However, we cannot
401 totally exclude the possibility that ^{13}C -enriched organic matter might have transferred
402 from the marine POC fraction to the DOC fraction during incubation. In fact, the DOC
403 $\delta^{13}\text{C}$ values was slightly increased (from -24.0 to -23.7‰), though there is no change in
404 the concentration of DOC during the incubation period at St. A. Future study should
405 conduct more precise experiments to confirm selective decomposition of riverine DOC
406 in bottom seawater.

407 It should be noted that caution may need to be paid on interpretation of the result
408 of this study. Chen et al. (2016) reported that lipids and proteinaceous compounds were
409 abundant in DOM extracted by PPL from algae, whereas tannin- and lignin-like
410 compounds were abundant in DOM extracted by PPL from terrestrial organic matter.

411 Thus, tannin- and lignin-like compounds might be selectively extracted by PPL from
412 terrestrial organic matter in this study. Because tannin and lignin show biorefractory
413 nature, DOM extracted by PPL from terrestrial organic matter must be more resistant to
414 microbial decomposition compared to bulk terrestrial DOM. Although the changes in
415 the $\delta^{13}\text{C}$ values of DOM during the incubation experiment indicates the decomposition
416 of terrestrial DOM extracted by PPL, our estimation of contribution of riverine DOM
417 decomposition to total DOM decomposition may be underestimated.

418

419

420 *4.3. Conclusions*

421 In this study, we found that the DOC decomposition may contribute to hypoxia
422 formation. The bottom DOC concentration was influenced by both phytoplankton and
423 river water, with the former likely having a stronger impact in the northwestern Ariake
424 Sea in summer. Nevertheless, we also found major contributions of riverine DOC
425 decomposition to total organic carbon decomposition at some stations. However, our
426 results on the contribution of riverine DOC to hypoxia formation may not be conclusive
427 because only a limited number of experiments were performed. Still, in previous studies,
428 the contribution of DOC to hypoxia formation was not accounted for (Wang et al. 2016;
429 Su et al. 2017), because the variation of DOC in most coastal seas is conservative
430 compared to that of POC (Wang et al. 2016). For this reason, the contribution of
431 riverine DOC decomposition to hypoxia formation has been ignored in several related
432 works. Our results show, however, that future studies should consider the contributions
433 of both riverine and marine DOC to hypoxia formation.

434

435

436 **Acknowledgments**

437 We express our deep thanks to Toshihiro Miyajima and Nobue Saotome (The
438 University of Tokyo) for their assistance with the stable isotope analysis. This study
439 was supported in part by JSPS KAKENHI grant no. 21K05748 to HT, and 21H02271,
440 21K12211, 18H03360 to TK. We are grateful to the editor and anonymous reviewers as
441 their comments helped us to greatly improve the manuscript.

442

443 **References**

444 Asmala E, Autio R, Kaartokallio H, Pitkänen L, Stedmon CA, Thomas DN (2013)

445 Bioavailability of riverine dissolved organic matter in three Baltic Sea estuaries and
446 the effect of catchment land use. *Biogeosciences* 10:6969–6986

447 Asmala E, Autio R, Kaartokallio H, Stedmon CA, Thomas DN (2014) Processing of
448 humic-rich riverine dissolved organic matter by estuarine bacteria: effects of
449 predegradation and inorganic nutrients. *Aquat Sci* 76:451–463

450 Bauer JE (2002) Carbon isotope composition of DOM. In: Hansell DA, Carlson CA
451 (ed) *Biogeochemistry of Marine Dissolved Organic Matter*. Academic Press,
452 Amsterdam, pp 405–453

453 Bianchi TS (2011) The role of terrestrially derived organic carbon in the coastal ocean:
454 A changing paradigm and the priming effect. *Proc Natl Acad Sci* 108 (49):19473–
455 19481

456 Broek TAB, Walkerc BD, Guildersona TP, McCarthy MD (2017) Coupled ultrafiltration
457 and solid phase extraction approach for the targeted study of semi-labile high
458 molecular weight and refractory low molecular weight dissolved organic matter.
459 *Mar Chem* 194:146–157

460 Chen CC, Gong GC, Shiah FK (2007) Hypoxia in the East China Sea: One of the
461 largest coastal low-oxygen areas in the world. *Mar Environ Res* 64:399–408

462 Chen M, Kim S, Park J-E, Kim HS, Hur J (2016) Effects of dissolved organic matter
463 (DOM) sources and nature of solid extraction sorbent on recoverable DOM
464 composition: Implication into potential lability of different compound groups. *Anal*
465 *Bioanal Chem* 408:4809–4819

466 Dai M, Yin Z, Meng F, Liu Q, Cai W-J (2012) Spatial distribution of riverine DOC
467 inputs to the ocean: an updated global synthesis. *Curr Opin Environ Sustain* 4:170–
468 178

469 Dickson AG (1994) Determination of dissolved oxygen in sea water by Winkler titration.
470 WOCE operations manual: the observational programme, section 3.1: WOCE
471 hydrographic programme, part 3.1.3: WHP operations and methods, vol 3. WHP
472 Office Report WHPO 91-1, WOCE Report No. 68/91 November 1994, Woods Hole.
473 Available at: [https://www.nodc.noaa.gov/woce/woce_v3/wocedata_1/whp/manuals.](https://www.nodc.noaa.gov/woce/woce_v3/wocedata_1/whp/manuals.htm)
474 [htm](https://www.nodc.noaa.gov/woce/woce_v3/wocedata_1/whp/manuals.htm) Accessed 18 March 2017

475 Diaz RJ, Rosenberg R (2008) Spreading dead zones and consequences for marine
476 ecosystems. *Science* 321:926–929

477 Dittmar T, Koch B, Hertkorn N, Kattner G (2008) A simple and efficient method for the
478 solid-phase extraction of dissolved organic matter (SPE-DOM) from seawater.
479 *Limnol Oceanogr Meth* 6:230–235

480 Deutsch B, Alling V, Humborg C, Korth F, Mörth CM (2012) Tracing inputs of
481 terrestrial high molecular weight dissolved organic matter within the Baltic Sea
482 ecosystem. *Biogeosciences* 9:4465–4475.

483 DeVilbiss SE, Zhou Z, Klump JV, Guo L (2016) Spatiotemporal variations in the
484 abundance and composition of bulk and chromophoric dissolved organic matter in
485 seasonally hypoxia-influenced Green Bay, Lake Michigan, USA. *Sci Total Environ*
486 565:742–757

487 Hansell DA, Carlson CA (2002) *Biogeochemistry of marine dissolved organic matter.*
488 first ed. Elsevier, Amsterdam

489 Hayami Y (2007) Hypoxic water mass in the inner area of the Ariake Sea: its formation
490 and inter-annual variation. *Monthly Kaiyo* 39(1):22–28 [in Japanese]

491 Hayami Y, Fujii N (2018) Decadal-scale variation in COD and DIN dynamics during
492 the summer in the inner area of the Ariake Sea, Japan. *J Oceanogr* 74(6):551–563

493 Ishita K, Fujiie W, Yanaga J, Takemoto M, Ono E, Shiratani E (2016) Influence of
494 wind-driven currents upon behavior of fresh water from Chikugo River in the inner
495 part of Ariake Bay. *J Jpn Soc Civ Eng B3-72*:688–693 [in Japanese with English
496 abstract]

497 Japan River Association: Rokkaku R, Kyushu RB (2002)
498 [http://www.japanriver.or.jp/river_law/kasenzu/kasenzu_gaiyou/kyushu_r/095rokkak](http://www.japanriver.or.jp/river_law/kasenzu/kasenzu_gaiyou/kyushu_r/095rokkaku.htm)
499 [u.htm](http://www.japanriver.or.jp/river_law/kasenzu/kasenzu_gaiyou/kyushu_r/095rokkaku.htm) Accessed March 2020

500 Jiao N, Robinson C, Azam F, Thomas H, Baltar F, Dang H, Hardman-Mountford NJ,
501 Johnson M, Kirchman DL, Koch BP, Legendre L, Li C, Liu J, Luo T, Luo YW,
502 Mitra A, Romanou A, Tang A, Wang X, Zhang C, Zhang R (2014) Mechanisms of
503 microbial carbon sequestration in the ocean—future research directions.
504 *Biogeosciences* 11:5285–5306

505 Lee B-G, Fisher NS (1992) Degradation and elemental release rates from phytoplankton
506 debris and their geochemical implications. *Limnol Oceanogr* 37:1345–1360

507 Lehmann MF, Bernasconi SM, Barbieri A, McKenzie A (2002) Preservation of organic
508 matter and alteration of its carbon and nitrogen isotope composition during
509 simulated and in situ early sedimentary diagenesis. *Geochim Cosmochim Acta*
510 66:3573–3584

511 Lewis CB, Walker BD, Druffel ERM (2020) Isotopic and optical heterogeneity of solid
512 phase extracted marine dissolved organic carbon. *Mar Chem* 219:103752

513 Lorrain A, Savoye N, Chauvaud L, Paulet YM, Naulet N (2003) Decarbonation and
514 preservation method for the analysis of organic C and N contents and stable isotope
515 ratios of low-carbonated suspended particulate material. *Anal Chimica Acta*
516 491:125–133

517 Ministry of Land, Infrastructure, Transport and Tourism: Iwayagawauchi Dam, Kawano
518 Bousai Jyouhou (2020a)
519 [https://www.river.go.jp/kawabou/ipDamPast.do?init=init&obsrvId=1049700700006](https://www.river.go.jp/kawabou/ipDamPast.do?init=init&obsrvId=1049700700006&gamenId=01-1103&fldCtlParty=yes)
520 &gamenId=01-1103&fldCtlParty=yes Accessed March 2020

521 Ministry of Land, Infrastructure, Transport and Tourism: Yokotake Dam, Kawano
522 Bousai Jyouhou (2020b)
523 [http://www.river.go.jp/kawabou/ipDamPast.do?init=init&obsrvId=1049700700011](http://www.river.go.jp/kawabou/ipDamPast.do?init=init&obsrvId=1049700700011&gamenId=01-1103&fldCtlParty=no)
524 &gamenId=01-1103&fldCtlParty=no Accessed March 2020

525 Peterson B, Fry B, Hullar M, Saupe S, Wright R (1994) The distribution and stable
526 carbon isotopic composition of dissolved organic carbon in estuaries. *Estuaries*
527 17:111–121

528 R Development Core Team: R (2017) A language and environment for statistical
529 computing. R Foundation for Statistical Computing, Vienna.

530 Raymond PA, Bauer JE (2001) DOC cycling in a temperate estuary: A mass balance
531 approach using natural ^{14}C and ^{13}C isotopes. *Limnol Oceanogr* 46:655–667

532 Redfield AC, Ketchum BH, Richards FA (1963) The influence of organisms on the
533 composition of seawater. In: Hill MH (ed) *The Sea*, vol. 2, Wiley, New York, USA,
534 pp 26-77

535 Rochelle-Newall EJ, Pizay MD, Middelburg JJ, Boschker HTS, Gattuso JP (2004)
536 Degradation of riverine dissolved organic matter by seawater bacteria. *Aquat*
537 *Microb Ecol* 37:9–22

538 Sato M, Takita T (2000) What bay is Ariake Bay? (Ariakekai towa donna tokoroka). In:
539 Sato M (ed) *Life in Ariake Bay (Ariakekai no ikimono tachi)*, Kaiyusha, Tokyo,
540 Japan, pp 9–31 [in Japanese]

541 Su J, Dai M, He B, Wang L, Gan J, Guo X, Zhao H, Yu F (2017) Tracing the origin of
542 the oxygen-consuming organic matter in the hypoxic zone in a large eutrophic
543 estuary: the lower reach of the Pearl River Estuary, China. *Biogeosciences* 14:
544 4085–4099

545 Takasu H, Uchino K (2021) Nutrient regeneration from riverine high-molecular-weight
546 dissolved organic matter through marine bacterial decomposition in a eutrophic
547 coastal system: The Ariake Sea, Japan. *J Sea Res* 177:102114

548 Tsutsumi H, Takamatsu A, Nagata S, Orita R, Umehara A, Komorita T, Shibamura S,
549 Takahashi T, Komatsu T, Montani S (2015) Implications of changes in the benthic
550 environment and decline of macro-benthic communities in the inner part of Ariake
551 Bay in relation to seasonal hypoxia. *Plankton Benthos Res* 10:187–201

552 Tokunaga T, Hayami Y, Kimoto K (2016) Biological and chemical oxygen consumption
553 above the sediments in the inner western part of Ariake Sea. *J Jpn Soc Civ Eng B2*
554 72:12–21 [in Japanese with English abstract]

555 Tokunaga T, Matsunaga N, Abe A, Kodama M, Yasuda H (2005) Field observations of a
556 high turbidity layer in western area of Ariake Sea and laboratory experiments of
557 oxygen consumption by suspended solids. *J Jpn Soc Civ Eng* 782:117–129 [in
558 Japanese with English abstract]

559 Uchino K, Inomata H, Tahara S, Takasu H (2019) Contribution of organic matter
560 decomposition in water column to oxygen consumption in the inner part of the
561 Ariake Sea. *J Jpn Soc Water Environ* 42:195–200 [in Japanese with English
562 abstract]

563 Uchino K, Mori K, Fukushima N, Takasu H (2021) Influence of river inflow and
564 microbial activity on distribution of dissolved organic carbon in the northern part of
565 Ariake Sea, Kyushu, Japan. *J Water Environ Technol* 19:153–160

566 Yamashita Y, Tanoue E (2003) Chemical characterization of protein-like fluorophores in
567 DOM in relation to aromatic amino acids. *Mar Chem* 82:255–271

568 Yoshino K, Yamada K, Kimura K (2018) Does suspended matter drained from the
569 Isahaya freshwater reservoir cause organic enrichment in the northern Ariake Bay? *J*
570 *Oceanogr* 74:619–62

571 Ward ND, Keill RG, Medeiros PM, Brito DC, Cunha AC, Dittmar T, Yager PL, Krusche
572 AV, Richey JE (2013) Degradation of terrestrially derived macromolecules in the
573 Amazon River. *Nature Geosci* 6:530–533

574 Wang H, Dai M, Liu J, Kao S, Zhang C, Cai W, Wang G, Qian W, Zhao M, Sun Z
575 (2016) Eutrophication-driven hypoxia in the East China Sea off the Changjiang
576 Estuary. *Environ Sci Technol* 50:2255–2263

577 Welschmeyer NA (1994) Fluorometric analysis of chlorophyll-a in the presence of
578 chlorophyll-b and pheopigments. *Limnol Oceanogr* 39:1985–1992

579 Zhang Y, Gao X, Guo W, Zhao J, Li Y (2018) Origin and dynamics of dissolved organic
580 matter in a mariculture area suffering from summertime hypoxia and acidification.
581 *Front Mar Sci* 5:32

582

583

584 **Table 1** Physical, chemical, and biological variables and concentrations and carbon
 585 stable isotope ratio ($\delta^{13}\text{C}$) of dissolved organic carbon (DOC) and particulate organic
 586 carbon (POC) and contribution of terrestrial DOC and POC at sampling sites in 2019.
 587

St.	Month	Bott. Depth (m)	DO Salinity (mg L ⁻¹)	Chl. <i>a</i> ($\mu\text{g L}^{-1}$)	DOC ($\mu\text{mo L}^{-1}$)	POC ($\mu\text{mo L}^{-1}$)	$\delta^{13}\text{C}$ -DOC (‰)	$\delta^{13}\text{C}$ -POC (‰)	Terrestrial DOC (%)	Terrestrial POC (%)	
St.1	May	5.7	27.8	5.6	7.6	125.7	57.5	-23.9	-25.5	47.7	65.9
	Jun	6.4	28.0	3.6	5.2	132.4	42.5	-23.2	-24.8	39.8	58.0
	Jul	4.8	28.0	4.0	15.9	102.4	34.1	-23.2	-24.6	39.8	55.7
	Aug	4.5	21.3	2.3	10.1	125.7	22.5	-23.0	-26.7	37.5	79.5
St.2	May	5.9	28.7	6.3	10.6	145.7	40.0	-23.6	-22.9	44.3	36.4
	Jun	6.0	29.6	3.3	10.7	91.6	22.5	-24.7	-22.6	56.8	33.0
	Jul	5.1	27.8	4.0	15.2	79.9	31.6	-22.7	-24.0	34.1	48.9
	Aug	5.0	25.4	5.6	11.6	142.4	26.6	-23.4	-24.3	42.0	52.3

588

589

590 **Table 2** Changes in concentrations (a) and $\delta^{13}\text{C}$ of DOC and POC and contribution of
 591 terrestrial DOC and POC during the experiments (a). TOC; sum of DOC and POC.

592 **a**

St.	DOC ($\mu\text{mo L}^{-1}$)			POC ($\mu\text{mo L}^{-1}$)			DOC decompo./
	Int.	Fin.	Decompo.	Int.	Fin.	Decompo.	TOC decompo. (%)
A	124.9	124.9	0.0	133.1	99.2	33.9	0
B	119.9	114.1	5.8	45.9	40.0	5.9	49.7
C	101.6	98.3	3.3	66.7	36.1	30.6	9.8
D	90.8	87.4	3.3	44.2	35.3	8.9	27.2
E	127.4	123.2	4.2	80.4	54.2	26.2	13.7

593

594 **b**

St.	$\delta^{13}\text{C}$ -DOC (‰)			$\delta^{13}\text{C}$ -POC (‰)			Terrestrial DOC (%)			Terrestrial POC (%)		
	Int.	Fin.	Dif.	Int.	Fin.	Dif.	Int.	Fin.	Dif.	Int.	Fin.	Dif.
A	-24.0	-23.7	+0.3	-26.6	-26.5	+0.1	48.9	45.5	-3.4	78.4	77.3	-1.1
B	-22.2	-23.5	-1.3	-20.9	-26.1	-5.2	28.4	43.2	+14.8	13.6	72.7	+59.1
C	-22.7	-23.2	-0.5	-23.4	-26.6	-3.2	34.1	39.8	+5.7	42.0	78.4	+36.4
D	-23.3	-22.9	+0.4	-24.3	-27.9	-3.6	40.9	36.4	-4.5	52.3	93.2	+40.9
E	-24.0	-23.2	+0.8	-22.6	-25.1	-2.5	48.9	39.8	-9.1	33.0	61.4	+28.4

595

596

597

598 **Figure legends**

599 **Fig. 1.** Maps of the Japanese islands (a), Kyushu Island (b), and the northern Ariake Sea
600 (c). Boxes indicate sampling stations in the Ariake Sea. The line indicates the horizontal
601 section mentioned in Fig. 2.

602

603 **Fig. 2.** Horizontal distribution of water temperature, salinity, seawater density ($\sigma\text{-t}$),
604 dissolved oxygen, and chlorophyll *a* (Chl. *a*). Black dots in the graphs indicate the
605 observation layers.

606

607 **Fig. 3.** Plots comparing salinity and the Chl. *a* concentration with dissolved organic
608 carbon (DOC) and particulate organic carbon (POC) concentrations. Circles and squares
609 indicate DOC and POC, respectively. Lines were fitted using linear regression, with the
610 regression results given in the plots.

611

612 **Fig. 4.** Changes in the natural carbon stable isotope ratio ($\delta^{13}\text{C}$) of DOC and POC
613 during the incubation experiment. Open and closed bars indicate DOC and POC,
614 respectively.

615

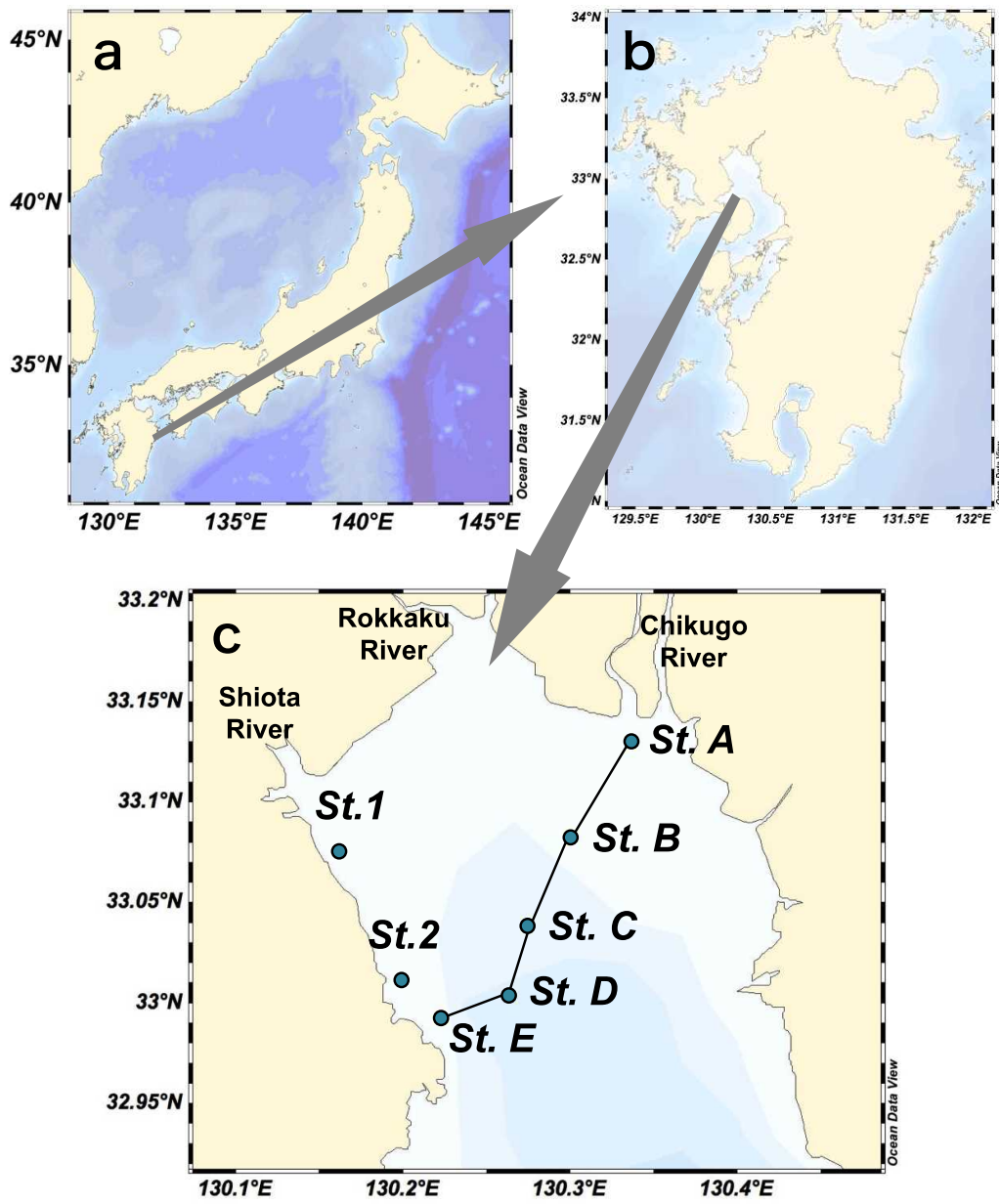


Fig. 1

616

617

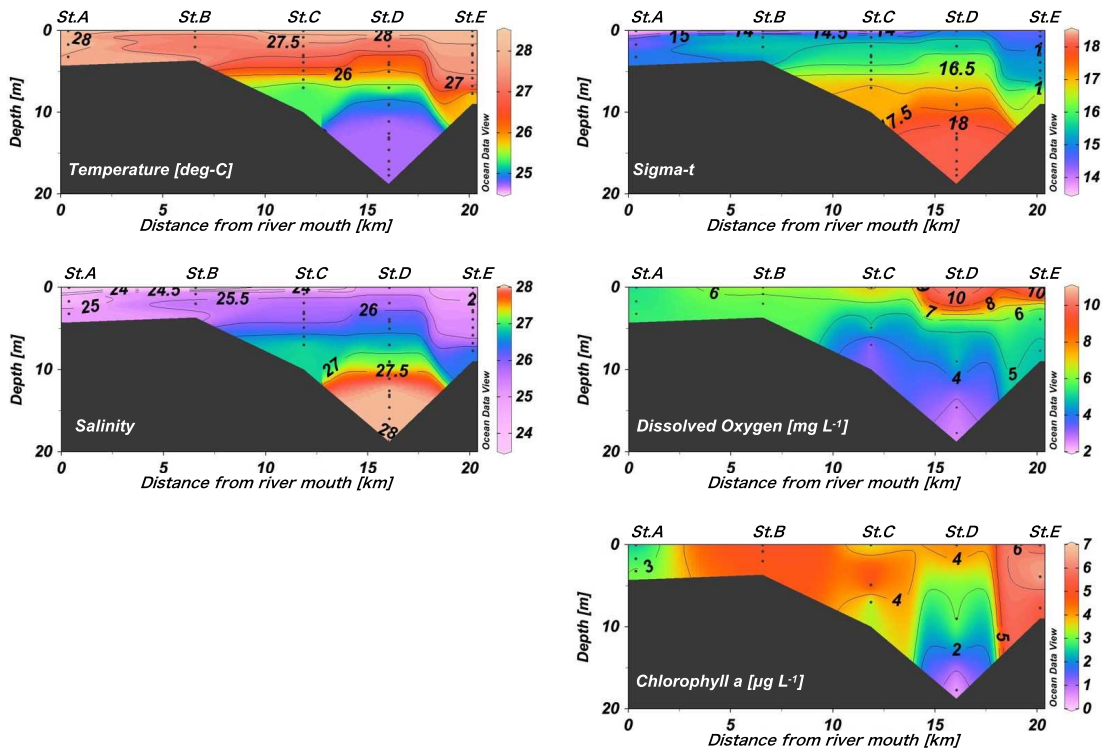


Fig. 2

618

619

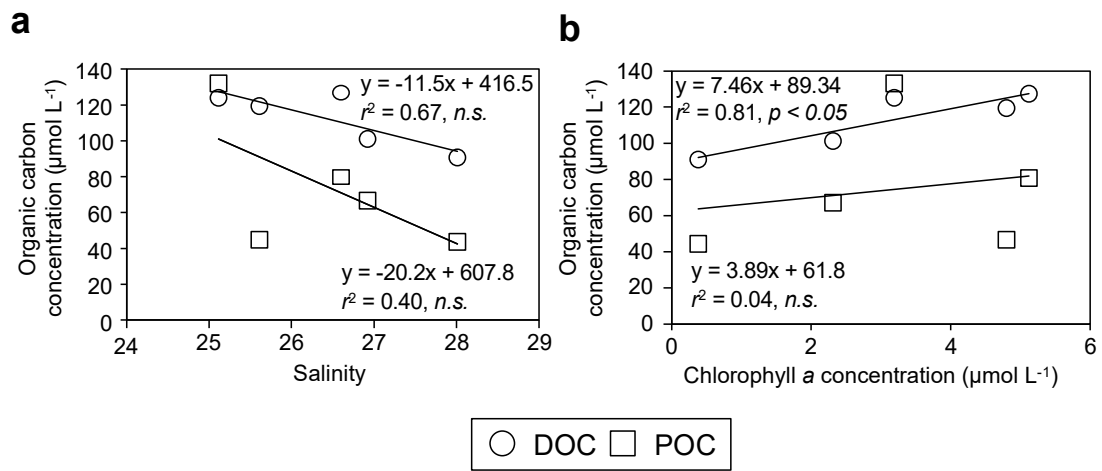


Fig. 3

620

621

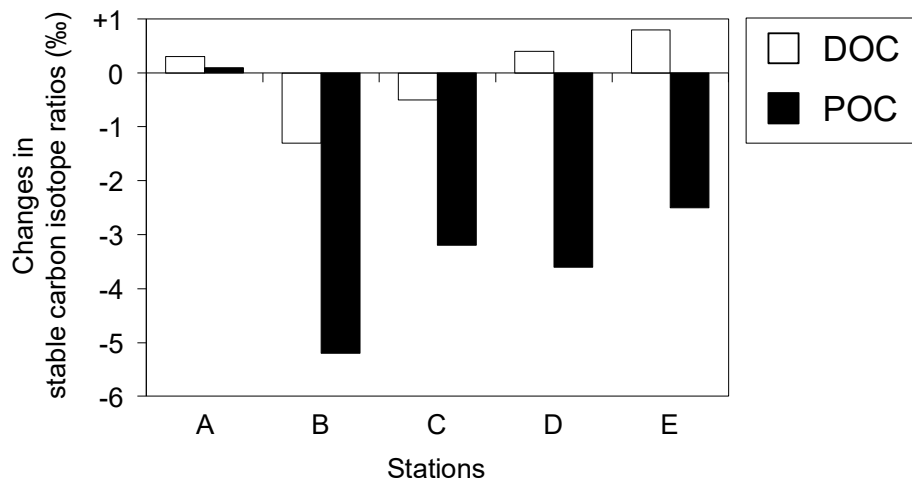


Fig. 4